Fuel 268 (2020) 117315

Contents lists available at ScienceDirect

Fuel

journal homepage: www.elsevier.com/locate/fuel

Full Length Article

Impact of pore morphology on two-phase flow dynamics under wettability alteration

Rimsha Aziz[a], Vahid Niasar[a,*], Hamidreza Erfani[a], Pedro J. Martínez-Ferrer[b]

[a] Department of Chemical Engineering and Analytical Science, University of Manchester, Oxford Road, Manchester M13 9PL, UK
[b] Centre for Mathematical Modelling and Flow Analysis, Chester Street, Manchester Metropolitan University, Manchester M1 5GD, UK

ARTICLE INFO

Keywords:
Low salinity waterflooding
Two-phase flow
Wettabillity alteration
Pore size distribution

ABSTRACT

Low salinity waterflooding aims to alter rock wettability from oil-wet towards less oil-wet or water-wet conditions. There is a limited understanding of how wettability alteration impacts two-phase flow, which is why it is unclear how wettability change impacts oil recovery. This study is an attempt to evaluate the effect of wettability alteration on two-phase flow for different pore size distributions under tertiary mode of low salinity waterflooding. Pore-scale, two-phase flow simulations with wettability alteration were performed in OpenFOAM's CFD tool. Two synthetic pore geometries (domains) were constructed with identical pore topology and connectivity, but different variances of pore throat radii. In our simulations, the pore network with a larger variance in pore radii resulted in 12% additional oil recovery. Whereas, the network with smaller variance in pore radii experienced no additional oil recovery despite the same wettability alteration change. This implies that change of wettability in clusters with a larger variation of pore radii can lead to a larger variation in capillary pressure gradient due to wettability alteration, which induces remobilisation of the trapped oil.

1. Introduction

Wettability is the ability of one immiscible fluid to wet the surface of the rock in the presence of another immiscible fluid [30]. Different wettability conditions lead to different fluid configurations within the pore space under equilibrium. For example, under water-wet condition, water is found around the grains and oil is found in the middle of the pore, the opposite occurs under oil-wet condition [30]. There are more complex wettability conditions, such as intermediate wettability (where both fluids have an equal affinity to the surface of the rock) and mixed wettability, where both oil and water-wet conditions can be found at the pore-scale at the same time [30]. Needless to say, change of wettability will cause a significant change in fluid's configuration at the pore-scale as well as its flow pattern [30,14,6]. Wettability is reported to be a function of i) composition of crude oil, ii) composition of brine (water initially found in the pore space), iii) rock mineralogy, also known as crude oil-brine-rock (COBR) system. The resultant force depending on the interaction of all three components establishes the final wettability state [30,48,29,38,5,25,17,12].

Under conventional waterflooding, wettability is thought to remain constant, however, under low salinity waterflooding where the salinity of the injected water is significantly reduced, wettability is known to shift towards less oil-wet (or more water-wet) conditions [38,6,5,26,21]. While, other mechanisms (e.g. visco-elastic interface, osmosis effect, interfacial reduction) are also observed under low salinity waterflooding, most researchers regard wettability alteration as the most notable effect [5,38,26,6,18,21]. The observation of wettability alteration under low salinity waterflooding is assumed to be a direct indicator of achieving higher oil recovery [5]. This assumption has been challenged in recent literature, where some studies have not reported higher oil recovery despite observing wettability alteration. Our current understanding of fluid dynamics in a porous medium is from high salinity waterflooding, where wettability is presumably constant; however, low salinity waterflooding behaves differently due to wettability alteration, leaving a clear gap in knowledge [7,6,26,4,3]. Our lack of understanding about how wettability alteration affects two-phase flow inhibits us from answering some critical questions such as, how does wettability alteration influence oil recovery? What is the optimum wettability alteration? What is the impact of wettability alteration on other factors known to influence oil recovery? Few studies have attempted to construct new pore-scale models to reduce this gap in knowledge [7,6,26,4,3,43,44]. Our previous study attempted to understand the impact of wettability change on two-phase flow dynamics at pore-scale [4]. However, in this study we aim to evaluate the role of pore size distribution on additional oil recovery due to wettability alteration.

* Corresponding author.
E-mail address: vahid.niasar@manchester.ac.uk (V. Niasar).

https://doi.org/10.1016/j.fuel.2020.117315
Received 15 August 2019; Received in revised form 24 January 2020; Accepted 2 February 2020

1.1. Pore-scale dynamics of low salinity waterflooding

There are two ways to inject low salinity water: secondary and tertiary modes. Secondary mode refers to the injection of low salinity water from the beginning of waterflooding [5]. Tertiary mode refers to the injection of low salinity water (wettability alteration) after residual oil saturation is established by high salinity waterflooding (constant wettability). In the literature, secondary mode of low salinity waterflooding has significantly improved the efficiency of waterflooding in many experimental studies [41,2,1,10,37,31,39,28]. This is because sweep efficiency is improved as oil is easily displaced by low salinity water due to being in continuous phase at the pore-scale. On the contrary, under the tertiary mode, oil is found as a discontinuous phase (oil ganglia) due to initial high salinity waterflooding. This induces greater difficulty for low salinity water to produce more oil in tertiary mode, hence reducing its potential [37]. Therefore, in some experimental studies tertiary mode has not reported any significant additional oil recovery, despite wettability alteration [37,31,10,7,5]. Although these explanations are consistent with our understanding of two-phase flow behaviour from a theoretical point of view; however, currently there is no direct evidence of this explanation. From the literature point view, oil recovery under the tertiary mode of low salinity waterflooding is more uncertain to a varied pore-scale situation present at the point of injection. Therefore, it requires more research to better understand the factors influencing oil recovery, to better overcome the drawbacks. This gap in knowledge cannot be addressed through sub pore-scale studies, which majority of the studies in literature are focused upon. Instead, pore-scale studies are a good starting point to begin understanding critical fluid dynamics under low salinity waterflooding [38,5,43,44].

Factors such as aspect ratio (ratio of pore body radii and pore throat radii), pore size distribution, oil banking, remobilisation of oil ganglia have known to impact fluid dynamics at pore-scale under waterflooding [8,5]. Under single phase flow higher variation of the pore size distribution (heterogeneous) leads to lower permeability, due to fewer pores contributing to flow [45]. Few studies have also evaluated the impact of absolute pore size on the two-phase flow and performance of waterflooding such that lower efficiency results as pore size distribution is more varied [42,15,27,22]. While single-phase flow is well understood, waterflooding efficiency and two-phase flow behaviours under various wettability conditions are known to a lesser extent. Hence, this study evaluates the impact of pore size distribution on the performance of high salinity waterflooding (no change in wettability) and low salinity waterflooding (wettability alteration) in the tertiary mode.

1.2. Mixing of high and low salinity water

Low salinity water and high salinity water are miscible, therefore, under the tertiary mode, low salinity water mixes with the already present high salinity water. The water topology under two-phase conditions can be divided into two regions, flowing regions (advection dominated) and stagnant or dead-end regions (predominately diffusion dominated) [11,4]. While low salinity water mixes with high salinity water within one injected pore volume, the stagnant regions retain high salinity water for many more pore volumes, due to the different time scales of the mixing mechanisms [3,4,20]. This mixing process limits the reach of low salinity water in the already present water saturation topology due to the presence of stagnant regions [11,19,20,3]. Due to mixing, flowing regions experience wettability alteration much earlier than stagnant regions, inducing local variation in wettability conditions. Induced wettability alteration at the capillary interfaces, destabilizes the saturation profile established under high-salinity waterflooding. As a result of the wettability alteration the capillary pressures at the main menisci (interfaces between oil and water) which change towards more water-wet, will assist water invasion to new regions during waterflooding, leading to the unique behaviour of water referred to as “pull/push” mechanism [4]. High salinity water from stagnant regions is “pushed” out of the oil-wet pores, which causes the oil to migrate towards bigger pores. While low salinity water is “pulled” into newer neighbouring pores of which entry capillary pressure is overcome by the modified wettability [4]. This causes a change in oil configuration at the pore-scale. This novel behaviour of water under induced wettability alteration in tertiary mode was first highlighted in our previous study [4].

In the mentioned study, it was shown that low salinity water flooding in the secondary mode is more favourable than the tertiary mode due to absence of stagnant region. However, in the tertiary mode, the destabilisation of capillary interfaces and pull–push behaviour leads to internal redistribution of oil and consequently a part of the redistributed oil will be produced.

In an effort to expand our current understanding of this mechanism, we test these conditions under different pore size distribution in this study. Pore size distribution (that controls the capillary pressure) and mixing (that controls the spatial distribution of wettability) are both important physical parameters, while to best of our knowledge they have not been studied in the context of low salinity waterflooding and we aim to provide novel insights to bridge this gap in understanding.

2. Methods

To investigate the role of pore size distribution, two geometries were constructed with identical topology (same connectivity of pore throats) with a narrower pore size distribution (homogeneous) and a wider pore size distribution (heterogeneous). The homogeneous domain has the mean pore size of 300 μm and standard deviation of 82 μm. The Heterogeneous domain has the mean pore size of 150 μm and the standard deviation of 113 μm. The maximum and minimum pore throat radii were constrained by the computational feasibility of the numerical technique. Wettability was changed as a function of water salinity. The initial wettability was set to oil-wet conditions with initially only oil present in the pore space. Low salinity water was injected under tertiary mode, while keeping injection rate and fluid properties the same.

Immiscible two-phase flow was modelled using volume of fluid (VOF) method, coupled with mass and momentum equations available in the OpenFOAM library [47], the same methodology had been successfully applied in previous two-phase flow studies at pore-scale [33,35,3,4,24]. VoF method offers a direct numerical two-phase flow smulations that can resolve sub pore-scale two-phase flow and transport processes. Also, since Navier–Stokes equations are used in this method, it allows using physical properties such as contact angle, interfacial tension, and viscosity, which cannot be easily achieved in other pore-scale models such as Lattice Boltzmann and smoothed-particle hydrodynamics.

2.1. Two-phase flow

VOF method is an interface reconstruction method, implemented in the OpenFOAM solver interFoam. This method is capable of simulating immiscible and incompressible two-phase flow in porous media [47,36]. The advantages of this scheme compared to the other methodologies were mentioned in our previous study [4]. The volume fraction (α) represents the fluid present in each computational cell: α_1 represents oil and α_2 ($\alpha_2 = 1 - \alpha_1$) represents water fraction. A sharp interface is constructed in between cells containing values of $0 < \alpha_1 < 1$. The volume fraction field is determined by the mass equation:

$$\frac{\partial \alpha_1}{\partial t} + \nabla\cdot(\alpha_1 \mathbf{u}) + \nabla\cdot(\alpha_1(1-\alpha_1)\mathbf{u}_r) = 0, \quad (1)$$

where $\mathbf{u}$ is velocity field and $\mathbf{u}_r = \mathbf{u}_1 - \mathbf{u}_2$ is the relative velocity at the interface between oil and water. A weighted function is used to calculate fluid properties at the interface:

$$\rho = \rho_1\alpha_1 + (1-\alpha_1)\rho_2, \tag{2}$$

$$\mu = \mu_1\alpha_1 + (1-\alpha_1)\mu_2, \tag{3}$$

where ρ_1 and μ_1 represent the density and viscosity of oil and ρ_2 and μ_2 represent the density and viscosity of water, respectively. Mass and momentum of the system are calculated using the following equations:

$$\frac{\partial \rho \mathbf{u}}{\partial t} + \nabla\cdot(\rho\mathbf{u}\mathbf{u}) = -\nabla p + [\nabla\cdot(\mu(\nabla\mathbf{u} + \nabla\mathbf{u}^T))] + \mathbf{F}_{sa}, \tag{4a}$$

$$\nabla\cdot\mathbf{u} = 0, \tag{4b}$$

where the body force is represented by $\mathbf{F}_{sa}$. Interfacial forces are included in the body force. The body force $\mathbf{F}_{sa}$ is defined as:

$$\mathbf{F}_{sa} = \rho\mathbf{g}\cdot\mathbf{n}_\mathbf{z} + \int_\Gamma \sigma\kappa\delta(x-x_s)\hat{\mathbf{n}}d\Gamma(x_s), \tag{5}$$

where Γ is the liquid-liquid interface and $\delta(x-x_s)$ is the Dirac delta function, κ is the interface curvature, and σ is the interfacial tension between the two fluids. The curvature of the interface is given by $\kappa = -\nabla\cdot\left(\frac{\nabla\alpha_1}{|\nabla\alpha_1|}\right)$ and the unit vector $\hat{\mathbf{n}}$ is defined as $\hat{\mathbf{n}} = \frac{\nabla\alpha_1}{|\nabla\alpha_1|}$.

2.2. Low salinity waterflooding

Low salinity water is miscible with high salinity water, as viscosity and density of water remains the same despite reduction of salinity. We solve mass fraction of water salinity (α_3) with the following equation:

$$\frac{\partial\alpha_3}{\partial t} + \nabla\cdot(\alpha_3\mathbf{u} - D_{2,3}\nabla\alpha_3) = 0, \text{ for}\Omega_{\alpha_2} \tag{6}$$

where α_3 is the scaled water salinity mass fraction. The low salinity is transported in water (α_2) using advection ($\nabla\cdot\alpha_3\mathbf{u}$) and diffusion terms ($\nabla\cdot(D_{2,3}\nabla\alpha_3)$). $D_{1,3} = 0$ is the diffusion matrix of water salinity (α_3) into oil (α_1), thus ensuring no concentration can diffuse into oil. Moreover, the term $D_{1,3}\nabla\alpha_1$ of the divergence guarantees a sharp interface between water salinity (α_3) and oil (α_1), as it does not allow flux through the interface into the oil due to $D_{1,3}$ being zero. The diffusion coefficient matrix for water salinity into water ($D_{2,3}$) was defined as $1\times10^{-9}\text{m}^2\text{s}^{-1}$ [26].

2.3. Wettability alteration

The contact angle is used to define the vector orthogonal to the contact line interface:

$$\hat{\mathbf{n}}\cdot\hat{\mathbf{n}}_s = \cos\theta, \tag{7}$$

where $\hat{\mathbf{n}}$ and $\hat{\mathbf{n}}_s$ are vectors normal to the fluid-fluid interface and solid wall, respectively. To induce wettability alteration, contact angle was made a function of the scaled water salinity. The mass of water salinity was scaled such that $\alpha_3 = 0$ represents low salinity water and $\alpha_3 = 1$ represents high salinity water in our model. The contact angle was assumed to be a linear function of the scale salinity between 0,1:

$$\theta = \theta_{HS} + \frac{(\alpha_3 - \alpha_{HS})\times(\theta_{LS} - \theta_{HS})}{(\alpha_{LS} - \alpha_{HS})}, \tag{8}$$

where θ_{HS} is contact angle at high salinity water (140°) and θ_{LS} is contact angle at low salinity water (60°). The exact contact angle under high and low salinity is based on a recent experimental study [46]. α_3 is the mass fraction of scaled water salinity for a given position and time. $\theta_{HS} = 140°$ corresponds to $\alpha_{HS} = 1$, emulating oil-wet conditions under high salinity water. $\theta_{LS} = 60°$ corresponds to $\alpha_{LS} = 0$ emulating water-wet conditions under low salinity water. Since our objective is to identify flow dynamics due to wettability alteration, we have assumed a linear behaviour. This modelling approach does not take into account the effect of different compositions of all components of COBR or the time required for wettability change. [28,26,46,25,12,17].

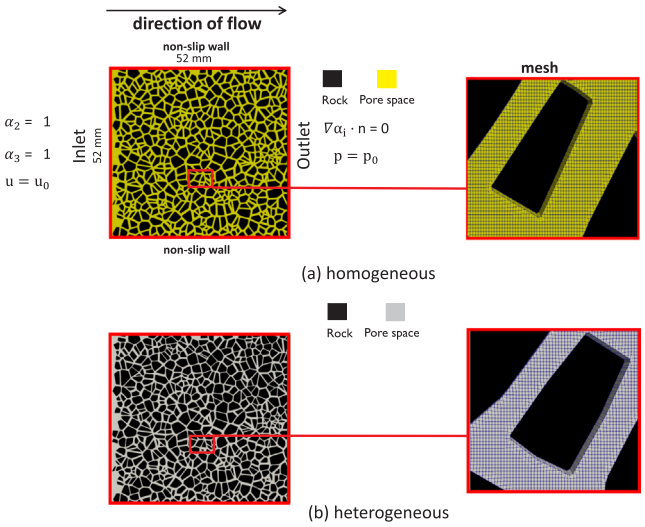

Fig. 1. Two-dimensional numerical domains: a) Homogeneous domain with mean pore size 300 μm with standard deviation of 82 μm. b) Heterogeneous domain with mean pore size 150 μm standard deviation of 113 μm. Water (α_2) and scaled water salinity (α_3) are initially zero in internal domain. Mesh for each domain is shown as inset.

2.4. Numerical schemes

Second-order discretisation schemes were used for spatial and temporal terms. Linear (central) interpolation was used for the evaluation of quantities at the cell faces from the cell centres and the van Leer limiter was used for the convection term to avoid numerical instabilities, whilst improving accuracy. The pressure was computed by coupling velocity and pressure [40]. Time-step (δt) was computed following the definition of the Courant number, $Co = \frac{\delta t\mathbf{u}}{\delta x} < 0.5$, where $\mathbf{u}$ represents the velocity and δx the cell size. The average time step during the simulation was 10^{-6} s.

2.5. Numerical domain, boundary, and initial conditions

Fig. 1 shows our numerical domains, have a square two-dimensional geometry. The homogeneous domain's mean pore size is 300μm with standard deviation of 82 μm. The heterogeneous domain's mean pore size distribution is 150 μm with standard deviation 113 μm. The geometries were generated by truncation log normal distribution and Voronoi concept to be representative of standstone. These geometries were synthetically constructed to provide a difference in pore size distribution, while preserving the same pore connectivity. Top and bottom boundaries were walls and share no-flow conditions with no-slip velocity. The right boundary was at constant pressure with zero gradient of scaled water salinity normal to the boundary. The left boundary had constant inlet injection velocity and constant scaled salinity value. The domain was initially fully saturated by the wetting phase (oil) with a contact angle of 140°. The velocity at the inlet was 0.009 ms^{-1}, which corresponds to a global capillary number of $Ca = 1\times10^{-4}$. The capillary number (Ca) is the ratio of viscous force relative to the capillary force:

$$Ca = \frac{\mu_w u_{in}}{\sigma}, \tag{9}$$

where u_{in} is inlet velocity of water, μ_w is viscosity of water and σ is interfacial tension. Smaller capillary numbers, which is more realistic of porous media flow, couldn't be applied in our study because OpenFOAM VOF method causes artificial velocities near the interface at that scale, which derives in mass conservation problems [35,24]. However, despite a higher capillary number, the capillary dominated flow dynamics are still observed in our study due to applying wettability

alteration after reaching steady-state water saturation under high salinity waterflooding.

The fluid properties used in the simulations were: water density (ρ_2) and viscosity (μ_2) as 998 kg m^{-3} and 10^{-3} kg $m^{-1}s^{-1}$ respectively. Oil density (ρ_1) and viscosity (μ_1) were 844 kg m^{-3} and 1.910×10^{-2} kg $m^{-1}s^{-1}$, respectively. The interfacial tension (σ) was 0.07 kg s^{-2}.

The domain was meshed with OpenFOAM utility called snappyHexMesh [47]. This tool ensures high-quality mesh even in the narrowest pore. Final grid resolution was chosen based on the sensitivity study performed on our previous study, where after performing a mesh sensitivity test we observed that at least 12–15 cells were required in the width of each throat to minimize error (less than 1%) while resolving the velocity and pressure under two-phase flow [3]. The sensitivity analysis of results as a function of mesh size was performed and reported in [4]. The domain was meshed such that the narrowest pore was at least 15 cells thick (0.9 and 0.65 million cells in internal mesh of homogeneous and heterogeneous domains).

Initially, the oil saturated domain was flooded with high salinity water with constant wettability, until steady-state water saturation was reached in both heterogeneous and homogeneous domains. After reaching steady-state water saturation, low salinity water was injected into both domains to allow mixing with originally established high salinity water topology. Using the local salinity of water, the wettability was altered from oil-wet (140°) to water-wet conditions (60°). Same number of pore volumes of low salinity water were injected at the end of the simulations in both domains.

3. Discussion

Flow dynamics are analysed in two sets of conditions in both homogeneous and heterogeneous domains: i) high salinity waterflooding under initial oil-wet conditions ii) low salinity waterflooding with wettability alteration (140° − 60°) under tertiary mode. The water saturation against injected pore volume for all simulations is shown in Fig. 2. High salinity waterflooding at the same injection rate produces 61% of initial oil in place, in the homogeneous domain, whereas the heterogeneous domain produces 3% less oil at the end of high salinity waterflooding (water saturation reaches steady-state). Note that the saturation drop in the homogeneous domain after breakthrough is due to the outlet boundary that allows $\nabla \cdot \alpha_2 = 0$. This causes oil back-flow due to pressure decrease in the domain after water breakthrough.

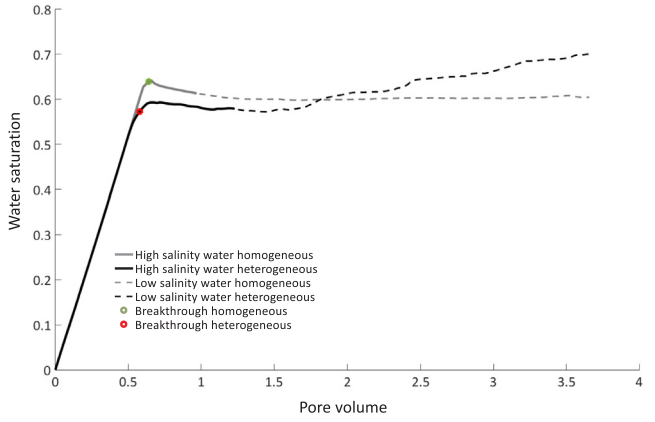

Fig. 2. Water saturation against injected pore volume for high salinity waterflooding (solid lines), low salinity waterflooding (dashed lines) for homogeneous (grey) and heterogeneous (black) domain for wettability alteration from 140° to 60°. High salinity waterflooding recovers higher oil recovery in homogeneous domain in comparison to heterogeneous domain due to more compact-front. However, under wettability alteration in low salinity waterflooding, 14% additional oil recovery was achieved in the heterogeneous case, but no additional oil recovery was achieved in the heterogeneous case.

3.1. Front dynamics under high salinity waterflooding

The impact of absolute pore sizes on two phase flow dynamics was largely evaluated under imbibition condition or single-phase flow in the literature [42]. Although relative permeability curves are produced for both imbibition and drainage conditions, very little is known about the dynamics of flow under these conditions apart from the displacement preference of the invading fluid in both processes. Our simulation results show that wider pore size distribution reduces the efficiency of waterflooding under drainage conditions. The homogeneous domain leads to 3% more oil production than the heterogeneous domain under high salinity waterflooding (refer to Fig. 2). The difference is not as significant as tertiary mode recovery. However, it indicates the difference in the fluid flow behaviour.

Under secondary waterflooding, when oil is found as a continuous phase, the oil recovery largely depends on displacement efficiency [15]. Through direct visualization and data analysis we have observed that the homogeneous domain has a higher permeability than the heterogeneous domain under drainage conditions. As a result of a narrower pore size distribution in the homogeneous domain, a uniform front is observed which leads to an increase in the sweep efficiency. In the heterogeneous domain, due to a wider pore size distribution, clear preferential flow pathways are observed which caused fingering during displacement of oil thus reducing sweep efficiency as 3% higher oil is bypassed. In Fig. 3 the distance travelled by the water front in both domains against water saturation is shown with snapshots of water topology at water saturations of 0.3 and 0.5. Since the length of the geometry and flow rate are the same for both cases, we can compare the distance travelled by the water front for a given saturation in both domains. Initially, the water front distance is not significantly different in both domains, in fact water front in the heterogeneous domain is lower than the homogeneous domain (refer to water saturation <0.3 in Fig. 3). However, for water saturation higher than 0.3, the preferential flow pathways become more evident in the heterogeneous domain (refer to Fig. 3 insert (b)). The preferential flow pathways have 3% higher velocity at water front in the heterogeneous domain compared to the homogeneous domain, that leads to fingering and subsequent earlier breakthrough. The recovery by high salinity waterflooding is in agreement with classical waterflooding behaviour, where most of the oil is recovered before breakthrough in the absence of film flow [30,15,16]. The role of spatial pore size distribution in viscous fingering has been also explored by a recent study [34].

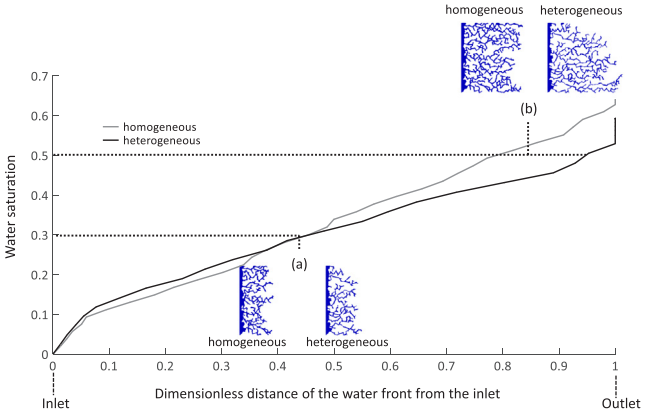

Fig. 3. Distance of water front from inlet, in the direction of flow is on x-axis, where 0 represent position of inlet and 1 represents position of outlet. Total water saturation is on y-axis for homogeneous (grey) and heterogeneous domain (black). The water topology at water saturation 0.3 is in insert (a) and 0.5 is in insert (b) for both heterogeneous and homogeneous domains.

3.2. Front dynamics under tertiary mode of low salinity waterflooding

Low salinity waterflooding in tertiary mode leads to 14% additional oil recovery in the heterogeneous domain, whereas the homogeneous domain leads to no additional recovery (refer to Fig. 2). Both domains experience the same wettability alteration but the heterogeneous domain displaces/remobilises significantly more oil under wettability alteration. Some experimental studies have reported no significant oil recovery despite wettability alteration; however, there is no understanding of why tertiary mode works in some cases and not in others [37,31,10,23]. The effect of pore size distribution on tertiary mode of low salinity waterflooding can be discussed from two aspects: i) mixing of low salinity water in high salinity water and ii) oil ganglia dynamics under heterogeneous and homogeneous pore size distributions, after induced wettability alteration.

3.2.1. Mixing, capillary instability and oil ganglia dynamics

Wettability alteration is affected by mixing of high and low salinity water under tertiary mode. In the tertiary mode, low salinity water dilutes the water in the pore space initially filled by the high salinity water and consequently the wettability changes. Previous studies of transport under two-phase flow conditions illustrated the transport within the water-filled area does not happen homogeneously and some regions are more advection controlled called flowing regions (blue in Fig. 4) and some other regions such as stagnant/dead-end regions (Red in Fig. 4) are predominantly diffusion controlled [19,20,9,3,13].

The flowing and stagnant regions of water topologies for both domains at the end of the high salinity waterflooding are shown in Fig. 4. These areas are identified based on concentration thresholding. After 1 pore volume of low salinity water injection, areas which are filled with low salinity water are labelled as flowing regions and the areas with no mixing are labelled as stagnant regions. Concentration threshold is used due to dynamic conditions (saturation topology changes over time) in which we can not use equilibrium velocity threshold established in our previous study [3]. Our previous study shows that it takes 1 pore volume injection for flowing regions to saturate with the inlet concentration. Therefore, after 1 pore volume injection of low salinity water, the regions filled with low salinity water were labelled as flowing and areas which retained the original high salinity water were labelled stagnant. The stagnant water saturation in the heterogeneous and the homogeneous domains are almost similar (0.08 and 0.07, respectively). When the low salinity water is injected into the porous media, the flowing regions experience wettability alteration at an earlier time scale than the stagnant regions. This causes local heterogeneous wettability alteration around the water topology, shown by Aziz et al. [4].

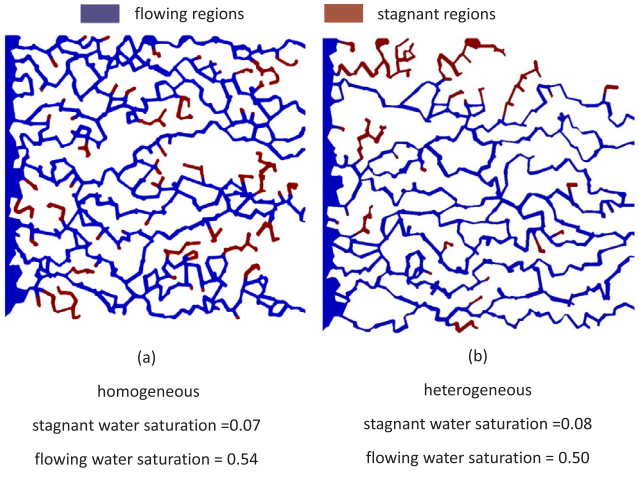

Fig. 4. Water topology at the end of high salinity waterflooding is shown for homogeneous (a) and heterogeneous (b) domains, classified into flowing (blue) and stagnant regions (red). Stagnant water saturation of heterogeneous is 0.08 and homogeneous domains is 0.07 of total water saturation.

Local heterogeneous wettability alteration leads to a fluid flow mechanism, referred to as “pull and push” demonstrated in our previous research [4]. Induced wettability alteration at the capillary interfaces destabilizes the saturation profile established under high-salinity waterflooding. As a result, the capillary pressures at the main menisci (oil water interfaces) changes towards more water-wet condition, which assists water invasion to new regions. Since stagnant regions are oil-wet, water would *pull* out from the dead-end regions and in some new regions water interfaces with wettability towards water-wet *push* the oil out of pores [4]. Our simulation results show that the presence of stagnant regions of water causes oil to divide into local ganglia. When water from stagnant regions *pull* out of the pores under heterogeneous wettability, local oil coalescence occurs. An example of this is shown in Fig. 5(a) and (b), where 3 ganglia are present (coloured as green, yellow and pink) with stagnant water (blue) in snapshot 1 and 2 for both domains. In snapshot (1) the oil ganglia and water stagnant region are at steady-state after high salinity waterflooding. At snapshot (2) wettability heterogeneity is created at the pore-scale after low salinity water injection. As a result, stagnant water is pulled out of the same pores in which oil later coalesces (oil filling event). This process occurs around all stagnant regions in water topology of the domains.

By identifying pores (in our case computational cells), which contained stagnant water under high salinity waterflooding, we could track the volume of stagnant water, which experiences oil filling event after low salinity invasion over time (indicative of “pull and push” behaviour of water). Due to oil coalescence, the interfacial area (oil water interface) in the porous medium decreases under low salinity waterflooding, compared to high salinity waterflooding at the same time as pull push is happening. Combining this data analysis, the change in oil filling saturation over time after low salinity waterflooding is plotted against the change in interfacial area over time in Fig. 5(c), for the homogeneous domain. A strong correlation between change in oil filling saturation in stagnant regions and the reduction of interfacial area over time is observed.

The correlation coefficient is a statistical measure indicative of whether two variables are related to each other. The interfacial area over time shows the correlation coefficient of -0.6 when compared to the oil filling saturation over time, indicating that these two events are correlated to some degree. Since the homogeneous domain produces no additional oil ($S_{w,HSW} = S_{w,LSW}$), the reduction in interfacial area under low salinity waterflooding is due to the oil coalescence caused by “pull and push” behaviour of water. The same behaviour is observed in the heterogeneous domain. Oil coalescence observed locally under low salinity waterflooding can theoretically lead to oil banking at a larger scale. This is a favourable process for oil recovery because when oil ganglia size increase, oil is displaced/mobilised more easily in porous medium, which increases the potential of recovering additional oil [32]. Earlier experimental studies have reported oil banking under wettability alteration [7,6]. Although coalescence of the oil ganglia can be a favorable process, in our simulation we did not observe the mobilisation of oil ganglia in the homogeneous case as induced pressure gradient in the oil phase did not overcome the entry capillary pressure of pores in contact.

3.2.2. Oil ganglia remobilisation and pore size distribution

Oil ganglia remobilisation potential is higher in the heterogeneous domain due to the local variation in capillary pressure at the pore-scale, caused by the variable pore throat sizes around the trapped oil. Fig. 6(b) and (c) show snapshots at pore-scale for both heterogeneous and homogeneous domains, respectively. In the heterogeneous domain, Fig. 6(b), snapshot (1), pore throats surrounding water under high salinity waterflooding are of different sizes, but in the homogeneous domain, Fig. 6(c) snapshot (1), high salinity water is surrounded by

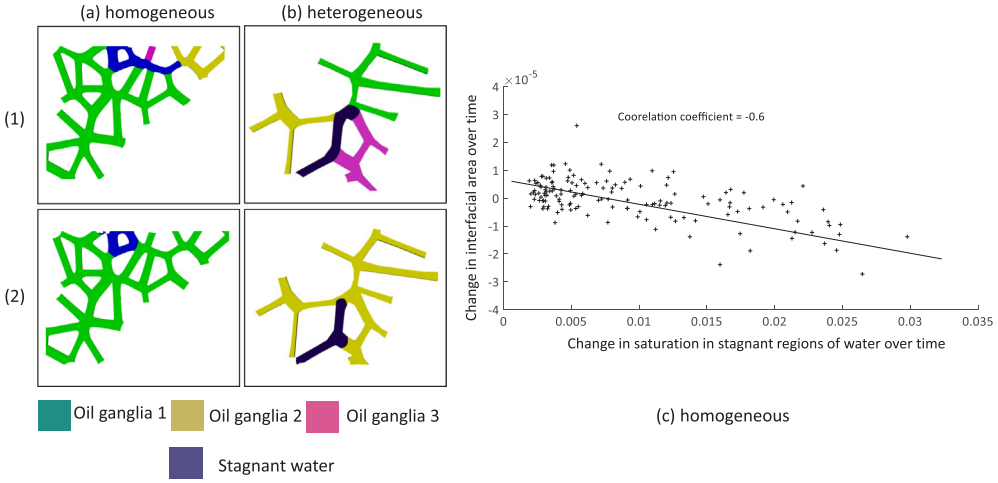

Fig. 5. At snapshot (1) 3 oil ganglia (green, yellow, pink) are shown at pore-scale in (a) homogeneous and (b) heterogeneous domains with stagnant water (blue) at steady-state saturation after high salinity waterflooding. At snapshot (2), the stagnant water is pulled out of these pores after low salinity waterflooding, as a result of local heterogeneous wettability. This "pull" behaviour of water causes oil coalescence. As a result of oil coalescence, interfacial area decreases in porous medium under low salinity waterflooding. When stagnant water is "pulled" out the pores, oil migrates to these pores which leads to oil filling events under low salinity waterflooding. We plot the change in water saturation in stagnant regions over time, against the change in interfacial area over time for (c) homogeneous domain under low salinity waterflooding.

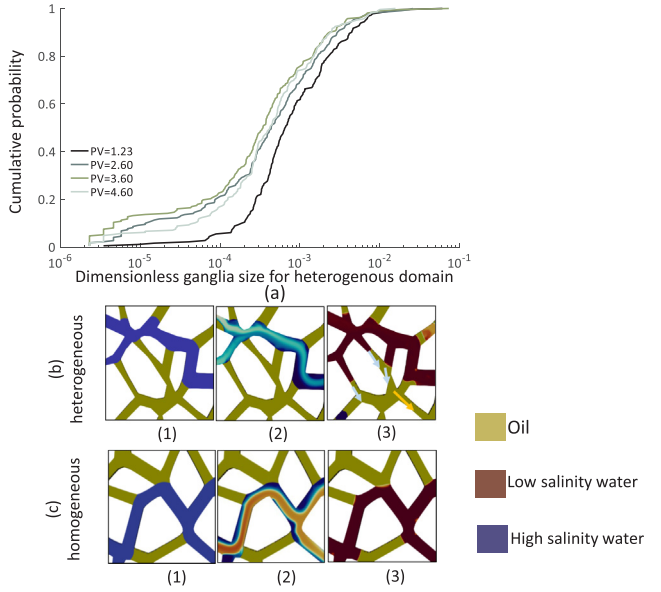

Fig. 6. a) Cumulative probability of oil ganglia size at four different pore volume/PV (1.23, 2.6, 3.60 and 4.60) in the heterogeneous domain. The plot shows the ganglia size initially decreasing and then increasing in the heterogeneous domain. b-c) Magnified pore-scale displacement of high salinity water (1) and low salinity water in transient (2) and low salinity water after wettability alteration (3) for the heterogeneous (b) and the homogeneous (c) domains. The yellow arrow shows the movement of oil (yellow) and light blue arrows shows the movement of low salinity water (dark red) which displaces newer pore throats.

pore throats of relatively similar sizes. At snapshot (2) mixing of low salinity water with high salinity water in both heterogeneous and homogeneous domains is observed. At snapshot (3) low salinity water has changed wettability in Fig. 6 (b) and (c). At snapshot (3) Fig. 6 (b), the oil is easily displaced in the heterogeneous domain. This is because after wettability alteration the variable pore size distribution leads to a pressure gradient in the oil ganglia which helps remobilisation. However, in the homogeneous domain, due to a narrower pore throat size distribution, the pressure under low salinity waterflooding around oil ganglia is fairly uniform. This results in further entrapment of oil at the pore-scale despite wettability alteration.

Our results show that under the tertiary mode of low salinity waterflooding, porous medium with wider pore size distribution is more favourable for oil recovery due to a varied local pressure induced through wettability alteration (i.e. local capillarity). Our study supports a different narrative to one presented in a recent pore network study of low salinity waterflooding under the same conditions [43]. This study acknowledged that while pore size distribution impacts the extent of oil recovery under low salinity waterflooding, however they concluded that a less varied pore size distribution will assist higher oil displacement due to more pores being invaded by the water as a result of wettability change [43]. The results of this pore network study are in direct contradiction to the results of our study, as under tertiary mode of low salinity waterflooding the alteration of wettability change will lower the capillary pressure to assist invasion. But it could also lead to further entrapment of oil ganglia since pore size distribution and wettability alteration may fail to create a sufficient pressure gradient within the ganglia, seen in Fig. 6(c) (3). These results now further raise a question, as to what extent of variation in pore size distribution is favourable for oil recovery under low salinity waterflooding in tertiary mode.

Oil coalescence caused by "pull and push" behaviour and the remobilisation of oil aids additional oil recovery in the heterogeneous domain. We show the oil coalescence behaviour before remoblisation in Fig. 6(c) for the heterogeneous domain. In Fig. 6(c) cumulative probability of dimensionless oil ganglia size is shown for pore volumes of 1.23, 2.60, 3.60 and 4.60. Fig. 6 (c) shows oil ganglia size decreasing monotonically between pore volume 1.23–3.60. However, at a pore volume of 4.60, the number of smaller size ganglia ($10^{-5} - 10^{-4}$) decreases and the number of bigger ganglia size ($10^{-3} - 10^{-2}$) increases, compared to the previous pore volume of 3.60. This indicates that smaller ganglia increase in size due to coalescence and then being displaced in the heterogeneous domain under low salinity waterflooding.

The lack of variability of pore sizes can potentially hinder the benefits of low salinity waterflooding despite wettability alteration under tertiary mode. These results further add to the debate that only wettability alteration is not sufficient to get favourable oil recovery at the pore-scale, but the effect of other parameters need to be investigated when predicting pore-scale conditions which can optimise the performance of low salinity waterflooding under tertiary mode. We would like to remark that this study is a preliminary work and, due to the computational cost and time, larger systems could not be simulated. However, it opens up a new discussion on the importance of geometrical and topological properties of the porous media in addition to the wettability alteration that can be investigated in future works.

Note that in our previous study [4] the redistribution of oil due to pull-push mechanism of water was deemed unfavourable for oil recovery as oil moved towards the bigger pores where it is further trapped

by the surrounding water-wet areas. This was highlighted in Fig. 5 of [4] where oil was observed to be redistributing internally. However, the remobilisation due to local variable capillary pressure observed in heterogeneous domain, in this study, forces oil out of equilibrium and constructs a clear path for oil to flow as a result of the heterogeneous pore size distribution. It also remobilises larger oil ganglia than the pull–push mechanism, which is why it has resulted in significant additional oil recovery. This study also show internally redistribution of oil in homogeneous domain where we observed no additional oil recovery due to the absence of local heterogeneity in pore size distribution. To summarise, remobilisation caused by wettability alteration under low salinity waterflooding in tertiary mode does not necessarily lead to higher oil recovery and our study strongly suggests that other factors such as pore size distribution, in addition, can have a more significant impact on the oil recovery.

4. Concluding remarks

Two-phase flow coupled with transport and wettability alteration was simulated in OpenFOAM. The objective of the study was to investigate the role of pore size distribution on low salinity waterflooding in tertiary mode, under wettability alteration. Two geometries were constructed with the same topology but different pore size distributions: heterogeneous (wider pore size distribution) and homogeneous (narrower pore size distribution). We evaluated the 2-phase flow dynamics under high salinity waterflooding and low salinity waterflooding under the tertiary mode and predefined that wettability could change from 140° to 60° with water salinity.

Based on our results, we conclude the following:

- The presence of stagnant water creates more oil ganglia locally: due to heterogeneous wettability conditions, stagnant water is pulled out of the pores causing oil coalescence/banking.
- The potential to remoblise oil in tertiary mode of low salinity waterflooding is higher for the heterogeneous domain due to a varied local pressure because of variation in the pore throat sizes and local capillary pressure.
- The efficiency of low salinity waterflooding does not depend only on the contact angle variation and pore morphology controls the ultimate performance. More spatial variability in capillary pressure may improve the ultimate performance in the tertiary mode.

Author contributions

RA performed the numerical simulations and data analysis. RA and VN defined the objectives of the study. VN led the research project. HEG created the geometries for the simulations. PJMF supported troubleshooting of OpenFOAM simulations and implemented the variable contact angle function. The manuscript was written through the contribution of all authors. All authors have given approval to the final version of the manuscript.

Data availability statement

The data will be made available upon publication on the IMPRES group website. (http://personalpages.manchester.ac.uk/staff/vahid.niasar/default.htm).

Declaration of Competing Interest

The authors declare that they have no known competing financial interests or personal relationships that could have appeared to influence the work reported in this paper.

Acknowledgment

We would like to acknowledge the UK Engineering and Physical Sciences Research Council (EPSRC) to provide the PhD studentship for Rimsha Aziz (EPSRC EP/M507969/1) and also American Chemical Society (ACS) New Direction Grant no 59640-ND9. We would also like to acknowledge the assistance given by IT Services and the use of the Computational Shared Facility at The University of Manchester. The authors would also acknowledge the University of Manchester for providing the PhD funding for Hamidreza Erfani through President's Doctoral Scholarship (PDS).

References

[1] Alagic E, Spildo K, Skauge A, Solbakken J. Effect of crude oil ageing on low salinity and low salinity surfactant flooding. J Petrol Sci Eng 2011;78:220–7.
[2] Ashraf A, Hadia N, Torsaeter O, Tweheyo MT. Laboratory investigation of low salinity waterflooding as secondary recovery process: effect of wettability. SPE Oil and Gas India Conference and Exhibition. Society of Petroleum Engineers; 2010.
[3] Aziz R, Joekar-Niasar V, Martinez-Ferrer P. Pore-scale insights into transport and mixing in steady-state two-phase flow in porous media. Int J Multiph Flow 2018;109:51–62.
[4] Aziz R, Joekar-Niasar V, Martínez-Ferrer PJ, Godinez-Brizuela OE, Theodoropoulos C, Mahani H. Novel insights into pore-scale dynamics of wettability alteration during low salinity waterflooding. Sci Rep 2019;9:9257.
[5] Bartels WB, Mahani H, Berg S, Hassanizadeh S. Literature review of low salinity waterflooding from a length and time scale perspective. Fuel 2019;236:338–53.
[6] Bartels WB, Mahani H, Berg S, Menezes R, van der Hoeven JA, Fadili A. Oil configuration under high-salinity and low-salinity conditions at pore scale: a parametric investigation by use of a single-channel micromodel. SPE J 2017;22:1362–73. https://doi.org/10.2118/181386-PA.
[7] Bartels WB, Rücker M, Berg S, Mahani H, Georgiadis A, Fadili A, Brussee N, Coorn A, van der Linde H, Hinz C. Fast x-ray micro-ct study of the impact of brine salinity on the pore-scale fluid distribution during waterflooding. Petrophysics 2017;58:36–47.
[8] Chatzis I, Morrow NR, Lim HT. Magnitude and detailed structure of residual oil saturation. Soc Petrol Eng J 1983;23:311–26.
[9] De Gennes P. Hydrodynamic dispersion in unsaturated porous media. J Fluid Mech 1983;136:189–200.
[10] Gamage S, Hasanka P, Thyne GD. Comparison of oil recovery by low salinity waterflooding in secondary and tertiary recovery modes. SPE Annual Technical Conference and Exhibition. Society of Petroleum Engineers; 2011.
[11] van Genuchten M, Wierenga P. Mass transfer studies in sorbing porous media. i. analytical solutions; 1976. p. 473–480.
[12] Godinez-Brizuela OE, Niasar VJ. Effect of divalent ions on the dynamics of disjoining pressure induced by salinity modification. J Mol Liq 2019;291:111276https://doi.org/10.1016/j.molliq.2019.111276.
[13] Hasan S, Joekar-Niasar V, Karadimitriou NK, Sahimi M. Saturation dependence of non-fickian transport in porous media. Water Resour Res 2019;55:1153–66.
[14] Jadhunandan P, Morrow NR. Effect of wettability on waterflood recovery for crude-oil/brine/rock systems. SPE Reservoir Eng 1995;10:40–6.
[15] Jerauld G. Prudhoe bay gas/oil relative permeability. SPE Reservoir Eng 1997;12:66–73.
[16] Joekar-Niasar V, Doster F, Armstrong R, Wildenschild D, Celia MA. Trapping and hysteresis in two-phase flow in porous media: a pore-network study. Water Resour Res 2013;49:4244–56.
[17] Joekar-Niasar V, Mahani H. Nonmonotonic pressure field induced by ionic diffusion in charged thin films. Ind Eng Chem Res 2016;55:6227–35.
[18] Joonaki E, Buckman J, Burgass R, Tohidi B. Water versus asphaltenes; liquid–liquid and solid–liquid molecular interactions unravel the mechanisms behind an improved oil recovery methodology. Sci Rep 2019;9:1–13.
[19] Karadimitriou NK, Joekar-Niasar V, Babaei M, Shore CA. Critical role of the immobile zone in non-fickian two-phase transport: a new paradigm. Environ Sci Technol 2016;50:4384–92. https://doi.org/10.1021/acs.est.5b05947, DOI: 10.1021/acs.est.5b05947.
[20] Karadimitriou NK, Joekar-Niasar V, Brizuela OG. Hydro-dynamic solute transport under two-phase flow conditions. Sci Rep 2017;7:6624.
[21] Karadimitriou NK, Mahani H, Steeb H, Niasar V. Nonmonotonic effects of salinity on wettability alteration and two-phase flow dynamics in PDMS micromodels. Water Resour Res.https://doi.org/10.1029/2018WR024252.
[22] Lacey M, Hollis C, Oostrom M, Shokri N. Effects of pore and grain size on water and polymer flooding in micromodels. Energy Fuels 2017;31:9026–34.
[23] Lager A, Webb KJ, Black C, Singleton M, Sorbie KS. Low salinity oil recovery-an experimental investigation1. Petrophysics 2008;49.
[24] Maes J, Geiger S. Direct pore-scale reactive transport modelling of dynamic wettability changes induced by surface complexation. Adv Water Resour 2018;111:6–19.
[25] Mahani H, Berg S, Ilic D, Bartels WB, Joekar-Niasar V. Kinetics of the low salinity waterflooding effect studied in a model system. Soc Petrol Eng 2013;9. https://doi.org/10.2118/165255-MS.
[26] Mahani H, Berg S, Ilic D, Bartels WB, Joekar-Niasar V. Kinetics of low-salinity-

flooding effect. SPE J 2015;20:8–20. https://doi.org/10.2118/165255-PA.
[27] Mayer AS, Miller CT. The influence of porous medium characteristics and measurement scale on pore-scale distributions of residual nonaqueous-phase liquids. J Contam Hydrol 1992;11:189–213.
[28] McMillan MD, Rahnema H, Romiluy J, Kitty FJ. Effect of exposure time and crude oil composition on low-salinity water flooding. Fuel 2016;185:263–72.
[29] Morrow N, Buckley J. Improved oil recovery by low-salinity waterflooding. J Petrol Technol 2011;63:106–12.
[30] Morrow NR. Wettability and its effect on oil recovery. J Petrol Technol 1990;42:1–476.
[31] Nasralla RA, Nasr-El-Din HA. Double-layer expansion: is it a primary mechanism of improved oil recovery by low-salinity waterflooding? SPE Reservoir Eval Eng 2014;17:49–59.
[32] Payatakes A. Dynamics of oil ganglia during immiscible displacement in water-wet porous media. Annu Rev Fluid Mech 1982;14:365–93.
[33] Rabbani HS, Joekar-Niasar V, Shokri N. Effects of intermediate wettability on entry capillary pressure in angular pores; 2016, p. 34–43.https://doi.org/10.1016/j.jcis.2016.03.053,http://www.sciencedirect.com/science/article/pii/S0021979716301953.
[34] Rabbani HS, Or D, Liu Y, Lai CY, Lu NB, Datta SS, Stone HA, Shokri N. Suppressing viscous fingering in structured porous media. Proc Nat Acad Sci 2018. 201800729.
[35] Raeini AQ, Blunt MJ, Bijeljic B. Modelling two-phase flow in porous media at the pore scale using the volume-of-fluid method. J Comput Phys 2012;231:5653–68.
[36] Rusche H. Computational fluid dynamics of dispersed two-phase flows at high phase fractions. Imperial College London (University of London); 2003. Ph.D. thesis.
[37] Shaker Shiran B, Skauge A. Enhanced oil recovery (eor) by combined low salinity water/polymer flooding. Energy Fuels 2013;27:1223–35.
[38] Sheng J. Critical review of low-salinity waterflooding. J Petrol Sci Eng 2014;120:216–24.
[39] Sorop TG, Masalmeh SK, Suijkerbuijk BM, van der Linde HA, Mahani H, Brussee NJ, Marcelis FA, Coorn A. Relative permeability measurements to quantify the low salinity flooding effect at field scale. Abu Dhabi International Petroleum Exhibition and Conference. Society of Petroleum Engineers; 2015.
[40] Springer J, Urban K, Kissling K, Schütz S, Piesche M, Jasak H. A Coupled Pressure Based Solution Algorithm Based on the Volume of Fluid Approach for Two or More Immiscible Fluids; 2010.
[41] Tang GQ, Morrow NR. Influence of brine composition and fines migration on crude oil/brine/rock interactions and oil recovery. J Petrol Sci Eng 1999;24:99–111.
[42] Wardlaw N, Cassan J. Oil recovery efficiency and the rock-pore properties of some sandstone reservoirs. Bull Can Pet Geol 1979;27:117–38.
[43] Watson MG, Bondino I, Hamon G, McDougall SR. A pore-scale investigation of low-salinity waterflooding in porous media: Uniformly wetted systems. Transp Porous Media 2017;118:201–23.
[44] Watson MG, McDougall SR. A mechanistic pore-scale analysis of the low-salinity effect in heterogeneously wetted porous media; 2019. arXiv preprint arXiv:1908.02874.
[45] Weger RJ, Eberli GP, Baechle GT, Massaferro JL, Sun YF. Quantification of pore structure and its effect on sonic velocity and permeability in carbonates. AAPG Bull 2009;93:1297–317.
[46] Wei B, Wu R, Lu L, Ning X, Xu X, Wood C, Yang Y. Influence of individual ions on oil/brine/rock interfacial interactions and oil?water flow behaviors in porous media; 2017. p. 12035–12045.
[47] Weller HG, Tabor G, Jasak H, Fureby C. A tensorial approach to computational continuum mechanics using object-oriented techniques. Comput Phys 1998;12:620–31.
[48] Yildiz HO, Morrow NR. Effect of brine composition on recovery of moutray crude oil by waterflooding. J Petrol Sci Eng 1996;14:159–68.